



HAL
open science

Reliable Risk Assessment and Management using Probabilistic Fusion of Predictive Inter-Distance Profile for Urban Autonomous Driving

Emmanuel Alao, Lounis Adouane, Philippe Martinet

► **To cite this version:**

Emmanuel Alao, Lounis Adouane, Philippe Martinet. Reliable Risk Assessment and Management using Probabilistic Fusion of Predictive Inter-Distance Profile for Urban Autonomous Driving. ECC 2024 - 22nd European Control Conference, Jun 2024, Stockholm, Sweden. hal-04525836

HAL Id: hal-04525836

<https://hal.science/hal-04525836v1>

Submitted on 28 Mar 2024

HAL is a multi-disciplinary open access archive for the deposit and dissemination of scientific research documents, whether they are published or not. The documents may come from teaching and research institutions in France or abroad, or from public or private research centers.

L'archive ouverte pluridisciplinaire **HAL**, est destinée au dépôt et à la diffusion de documents scientifiques de niveau recherche, publiés ou non, émanant des établissements d'enseignement et de recherche français ou étrangers, des laboratoires publics ou privés.

Reliable Risk Assessment and Management using Probabilistic Fusion of Predictive Inter-Distance Profile for Urban Autonomous Driving

Emmanuel Alao^{1,2}, Lounis Adouane¹ and Philippe Martinet²

Abstract—Autonomous driving in urban scenarios has become more challenging due to the increase in Personal Light Electric Vehicles (PLEVs). PLEVs correspond mostly to electric devices such as gyropods and scooters. They exhibit varying velocity profiles as a result of their high acceleration capacity. Multiple hypotheses about their possible motion make autonomous driving very difficult, leading to the highly conservative behavior of most control algorithms. This paper proposes to solve this problem by performing a continuous risk assessment using a Fusion of Predictive Inter-Distance Profile (F-PIDP). Then a stochastic MPC algorithm performs effective risk management using the F-PIDP while taking into account adaptive constraints. The advantages of the proposed approach are demonstrated through simulations of multiple scenarios.

I. INTRODUCTION

Considerable efforts have been channeled into the development of motion planners for Autonomous Driving Systems (ADS) with the aim of bolstering road safety. Nevertheless, the proliferation of novel multimodal transportation solutions in urban areas is either a direct or indirect cause of a rapid increase in the unpredictability of traffic environments. Subsequently, these novel multimodal transportation systems will be referred to as Personal Light Electric Vehicles (PLEVs). Examples of PLEVs are gyro-pods, monowheels, hoverboards, and electric scooters. Unexpected events often arise due to the unpredictable behaviors of pedestrians, whether or not they use PLEVs and adhere to traffic rules, since there are always multiple hypotheses on their future motion. Estimating the future states of the entities of interest in a traffic environment corresponds to a motion prediction problem, which is required to perform risk assessment and risk management for the safe navigation of autonomous vehicles among PLEVs. Many solutions to the motion prediction problem exist in the literature, such as the single model and multimodel method [1] for motion prediction. For instance, the popular interacting multiple models (IMM) approach [2] can consider numerous hypotheses on the future trajectory of a traffic participant. However, accounting for multimodal predictions makes risk assessment and management very challenging for most autonomous navigation algorithms as a result of the complexity of the number of possible trajectories. This directly increases the constraints on the motion of the ego-vehicle, leading to highly conservative behaviors. The most intuitive way to perform risk assessment during

real time operations of an ego-vehicle is to perform collision checks. This approach starts by predicting the future configuration of the ego-vehicle and the PLEVs in the environment before evaluating the configurations in which collision occurs. Other than computing where and when a collision occurs, some complex methods can be used to also evaluate the probability and the level of severity of the collision [3], [4]. Many collision-based risk assessment metrics have been proposed and leveraged in the literature, authors in [5] give a summary of the state of the art on criticality metrics and the relationship between them with regards to desired applications. Similarly, multiple performance metrics are presented in [6] for evaluating an autonomous vehicle moving in a shared space with pedestrians. The Time To Collision (TTC) [7] is the most popular risk indicator because of its simplicity and computational efficiency. TTC outputs the minimum time that collision could occur between two traffic participants (ego-vehicle and/or PLEVs) according to a given motion model. For vehicles, TTC can give a good estimate of the temporal proximity between vehicles in a well-defined scenario like the leader-follower configuration along a straight line [8]. However, TTC performs poorly even in common 2D situations like a curve intersection [9]. Extensions of the TTC have been proposed to solve this problem, such as the Extended Time to Collision (ETTC) in [10]. For PLEVs, an extension of the TTC referred to as time-to-x (TTX) in [11] computes a discrete time approximation of the time-to-collision, time-to-brake (TTB) and time-to-steer (TTS). In [12] a novel approach using a Predictive Inter-Distance Profile (PIDP) was applied for risk assessment as a spatio-temporal metric. The possibility of a collision happening is not always sure, due to the various uncertainties in the factors that influence the traffic environment. Hence, various probabilistic frameworks have been proposed in the literature for risk assessment, such as the Hidden Markov Model (HMM) employed in [9] and the Dynamic Bayesian Network (DBN) applied in [4] to measure the risk of performing multiple vehicle maneuvers. Reachability analysis [13] is another trending method for risk management in the research community.

Risk management methods are required for controlling or minimizing the level of risk in the road traffic, based on appropriate risk metrics. For example, using PIDP, the authors in [12], proposed to minimize the risk of collision using an adaptive PD controller combined with a neuro-fuzzy system for safe and flexible navigation. Model Predictive Control (MPC) is a similar method that is well known for its ability to consider the future behavior of the traffic participants

¹Université de Technologie de Compiègne (UTC), CNRS, Heudiasyc, Compiègne, France

{emmanuel.alao, lounis.adouane}@hds.utc.fr

²Centre Inria d'Université Côte d'Azur, (INRIA), ACENTAURI, Sophia Antipolis, France philippe.martinet@inria.fr

with constraints on the control inputs over a given time horizon [14]. MPC is not efficient for nonlinear dynamic motions with uncertainties. Stochastic MPC (SMPC) [15] is an extension of MPC method that represents the uncertainties in the navigation problem as chance constraints, modeled using a probabilistic distribution. Machine learning methods [16] have also been explored for risk assessment and management of autonomous vehicles. Using Deep Neural Networks (DNN) the authors in [17] were able to perform End-to-End (E2E) prediction and control of the velocity and steering of an ego-vehicle, whereas the authors in [18] perform image-based control using a combination of Convolutional Neural Networks (CNN) [19] and Long Short-Term Memory (LSTM) [20].

In this paper, we present a new risk assessment method called Fusion of PIDP (F-PIDP) that extends the traditional PIDP to account for uncertainties in the future trajectories of a PLEV. The proposed method takes advantage of the spatio-temporal characteristic of the PIDP and the robustness of multi-modal motion prediction methods. A combination of the proposed F-PIDP and SMPC algorithm is then used for risk management to mitigate possible collisions and ensure a smooth motion of the autonomous vehicle for the comfort of passengers and other traffic participants.

This paper is organized as follows. Section II, presents the backgrounds on the ego-vehicle model, multi-pedestrian motion model, and PIDP for risk assessment and management in the presence of PLEVs. The proposed F-PIDP for risk assessment is presented in Section III. In Section IV, we present the results of applying the proposed method in two possible scenarios. Finally, Section V concludes and highlight the main contributions of this paper.

II. BACKGROUND

A. Ego Vehicle Model

This section defines the model of the ego vehicle for the proposed risk assessment and management strategy. The kinematic bicycle model [21] is adopted to describe the motion of the vehicle because it only requires the essential (linear velocity and steering) control inputs of the vehicle, making it useful for quick planning and re-planning which is essential during the analysis of the proposed method [22].

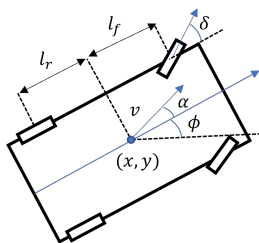


Fig. 1. The kinematic bicycle model for the prediction of the vehicle future states with the center of mass at (x, y)

The nonlinear bicycle model of the vehicle is expressed as:

$$\dot{x} = v \cos(\phi + \alpha) \quad (1)$$

$$\dot{y} = v \sin(\phi + \alpha) \quad (2)$$

$$\dot{\phi} = v/l_r \sin(\alpha) \quad (3)$$

$$\text{with, } \alpha = \arctan\left(\frac{l_r}{l_r + l_f} \tan \delta\right)$$

where $[\dot{x}, \dot{y}, \dot{\phi}]$ denotes the dynamic motion of the vehicle center. The linear velocity v and the steering δ are the control inputs $\mathbf{u} = [v, \delta]$ to the ego vehicle. Parameters l_r and l_f are respectively the length of the rear and front wheel to the center of the vehicle (cf. Figure 1).

B. Probabilistic Multi-Pedestrian Motion Model

This paper assumes that there are multiple trajectories that the PLEV can take based on the situation in the environment. Therefore, for every possible maneuver or mode, a trajectory is computed that represent the future motion. This approach supports making multiple hypotheses about future predictions with the same or varying levels of probability (cf. Figure 2). The probability of the trajectories may be determined by the uncertainty in the filter (e.g. IMM algorithm [2]) or directly from the sensors used. This approach accommodates multiple (model-based and machine learning-based) perception inputs, as long as the uncertainty in each trajectory is known. It is important to mention that the focus of this paper is on the proposed multi-risk assessment and management strategy (cf. Section III). All that is linked to the different probabilities attributed to the possible PLEV's trajectories as well as the perception aspects are directly inspired by the large literature on motion prediction [1].

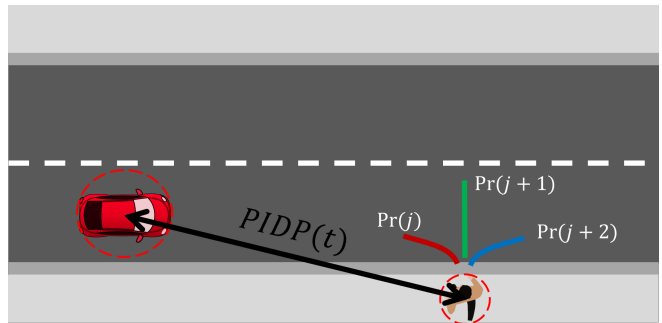


Fig. 2. Ego vehicle and a Jaywalking PLEV with multimodal trajectories: each trajectory has its own probability

C. Predictive Inter-distance Profile (PIDP)

PIDP is a metric used to assess the risk of collision between two or more traffic participants [10], [23]. The PIDP is essentially a projection of the inter-distance between these two entities, assuming their future trajectories are known and maintained during a certain time horizon, $t_{horizon}$. It is a risk assessment metric that can perform both time-scale and distance-scale measurement for continuous monitoring of the dangerous situations between two traffic participants over the given time horizon. PIDP is independent of the shape of

the trajectories of the interacting agents [12], which makes it appropriate for situations involving PLEVs. The primary objective of any control strategy in autonomous navigation is to maintain a safety distance. In the context of PIDP, this means ensuring that the computed inter-distance between the ego vehicle and the PLEV is consistently maintained above a predefined safety distance, represented as d_{safe} (cf. Figure 3). Collision occurs when the PIDP is less than the sum of the radius of the circle around the ego-vehicle and PLEV (i.e. $PIDP(t) \leq R + r$). However, since the motion of the PLEV is assumed to be multi-modal with probabilities, the typical PIDP is not sufficient for risk assessment in this context, hence the need for a fusion of PIDPs (F-PIDPs) defined in section III.

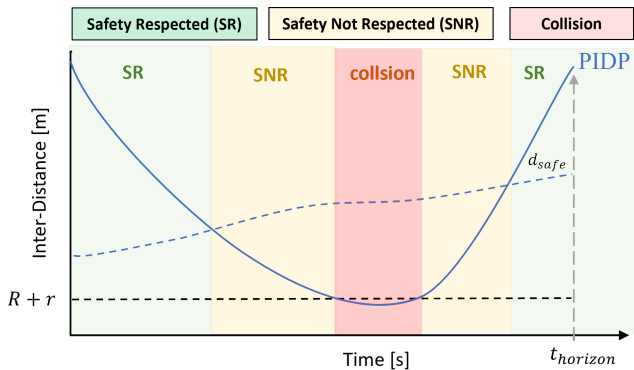


Fig. 3. Predictive Inter-Distance Profile (PIDP) between an ego-vehicle and a PLEV with the severity of the situations (SR: Safety Respected, SNR: Safety Not Respected, and Collision) w.r.t. the safety distance d_{safe} over the time horizon

III. FUSION OF PIDPs (F-PIDP) FOR CONTINUOUS RISK ASSESSMENT AND MANAGEMENT

Multimodal model of the pedestrian motion implies that there are multiple PIDPs for each pedestrian, either due to the uncertainty in the intended trajectories or the true velocity of the PLEV (cf. Figure 4). This increases the complexity of the navigation problem since each predicted trajectory is equivalent to a virtual PLEV with a probability of existence. The authors in [12] similar to many research studies solely focus on a single trajectory which is equivalent to selecting only the most probable trajectory, that is, the trajectory with the highest probability. But considering a single trajectory often fails because PLEV can rapidly switch its behaviors like accelerating its speed. Another control strategy is to only consider the most dangerous trajectory, that is, the trajectory with the smallest inter-distance. Such a strategy would lead to a highly conservative behavior. We propose to solve this multi-risk problem by performing a weighted fusion of the PIDPs. Therefore, using a quadratic polynomial curve with probabilistic weights, we obtain a Fusion of PIDPs (F-PIDP). The following subsections give a detailed explanation of the steps for computing the F-PIDP.

A. Computation of each PIDP

The first step is to compute the PIDP of each probable trajectory. Given a set of possible future trajectories of a PLEV, $\mathcal{P} = \{p_1, p_2, \dots, p_m\}$. The aim is to compute the magnitude of the distance vector between the future position of the ego-vehicle and the position of the PLEV at each time step t , if $r(t) = [x(t), y(t)]^T$ and $r_{p_j}(t) = [x_{p_j}(t), y_{p_j}(t)]^T$ are the position vectors of the vehicle and the j^{th} PLEV trajectory respectively. Then

$$PIDP_j(t) = \{d_j(t) | p_j \in \mathcal{P}, 0 \leq t \leq t_{horizon}\} \quad (4)$$

$$d_j(t) = \|r(t) - r_{p_j}(t)\| \quad (5)$$

here $PIDP_j$ denotes the inter-distance between the ego-vehicle and PLEV's j^{th} trajectory, obtained by calculating their Euclidean norm $\|\cdot\|_2$.

B. Parameterization of each PIDP

In general, the inter-distance profile is a nonlinear function due to the changing motion of the ego-vehicle and PLEV. Hence, important characteristics of each PIDP are extracted, to perform a fusion of the PIDPs and maintain a smooth curve. The extracted parameters from each $PIDP_j$ are:

- $PIDP_j(t_0)$ represents the start point of the j^{th} PIDP, which is the same for all probable trajectories
- $minPIDP_j(t_{min})$ the minimum of each PIDP at time t_{min} (cf. Figure 4)
- $PIDP_j(t_{horizon})$ the PIDP at the end of each predicted trajectory

C. PIDP fusion using probabilistic weights

The fusion step in the F-PIDP process combines multiple PIDPs into one representative prediction based on their level of uncertainty. In an ideal situation where the motion or velocity profile of the ego-vehicle and PLEV follow a smooth path, the PIDP is expected to be a quadratic polynomial curve derived from the Euclidean distance. Therefore, the parameters of all the PIDPs are fused together to form a single quadratic polynomial curve. From the equations of a quadratic polynomial:

$$d(t) = a_0 + a_1t + a_2t^2 \quad (6)$$

$$\begin{bmatrix} d(t_0) \\ \vdots \\ d(t_N) \end{bmatrix} = \begin{bmatrix} 1 & t_0 & t_0^2 \\ \vdots & \vdots & \vdots \\ 1 & t_N & t_N^2 \end{bmatrix} \cdot \begin{bmatrix} a_0 \\ a_1 \\ a_2 \end{bmatrix} \quad (7)$$

where $d(t_k)$ denotes the PIDP at time t_k and $\{a_0, a_1, a_2\} \in \mathbb{R}$ are parameters of the polynomial curve to be calculated. The parameters of this curve are determined

by calculating the probabilistic center of mass (pCoM) of all PIDPs. The probability based center of mass is defined as:

$$pCoM(t) = \sum_{j=1}^{N_{traj}} Pr(j) * d_j(t) \quad (8)$$

here, $N_{traj} \in \mathbb{R}$ denotes the number of predicted trajectories, $Pr(j)$ and d_j denotes the probability and inter-distance of the j^{th} predicted trajectory at the desired time t (i.e. start, minimum, and endpoint) of the PIDPs. This center of mass is a weighted average that considers the likelihood of each trajectory. The desired control points to find the parameters of the polynomial are the fusion of PIDP (F-PIDP):

- $F_PIDP(t_0)$ fusion of the initial points $PIDP_j(t_0)$, which is the same for all PIDPs
- $F_PIDP(t_{min})$ the fusion of all the minimum PIDPs $minPIDP_j(t_{min})$ based on pCoM
- $F_PIDP(t_{horizon})$ the fusion of all the final points $PIDP_j(t_{horizon})$

Since the fusion of the feature points $d(t)=F_PIDP(t)$ in (7) are known, the parameters of the fusion $\{a_0, a_1, a_2\}$ can be solved for using the matrix (or pseudo) inverse. The resulting parameters are then substituted in (6) to get a single unified F-PIDP curve that encapsulates the combined information as shown in Figure 4.

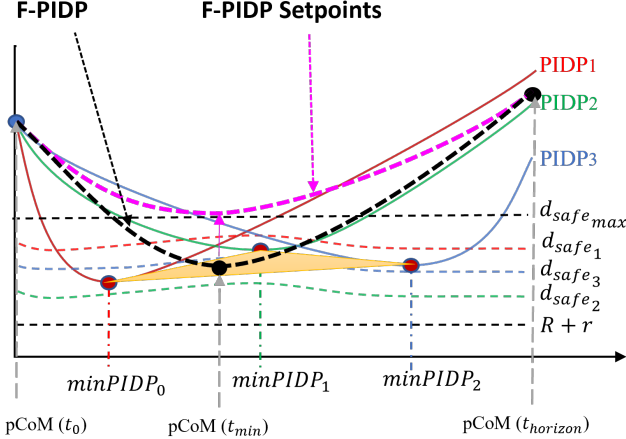


Fig. 4. Fusion of PIDPs (F-PIDP) of an ego-vehicle and a PLEV with multi-modal trajectories

D. PIDP Setpoint based on Safety Distance

After fusion, the base of the curve may fall below the maximum safety distance, indicating a risk of collision. The setpoint translation step ensures that the fused PIDP adheres to safety standards in the future PIDP. This is done by shifting the base of the curve vertically to meet or exceed the maximum safety distance. This implies that:

$$F_PIDP(t_{min}) \triangleq \max\{F_PIDP(t_{min}), d_{safe_{max}}\} \quad (9)$$

$$d_{safe_{max}} \triangleq R + r + v_{max} * ETTC(1sec) \quad (10)$$

where $d_{safe_{max}}$ is the maximum safety distance derived from the maximum velocity of the ego vehicle v_{max} and the extended time to collision ($ETTC$) of 1 seconds. R and r corresponds to the radius of the circle that surround completely the ego vehicle and PLEV respectively.

The new curve obtained after the translation (cf. Figure 4) serves as a reference to the SMPC algorithm and guarantees that the predicted trajectory maintains a safe separation from potential obstacles. By establishing a setpoint equal to or greater than the safety distance, collision risks are minimized. This step is therefore crucial for proactive and preventive navigation.

E. SMPC for Risk Management

SMPC is proposed to perform risk management by computing the optimal control actions of the ego-vehicle while accounting for various constraints and uncertainties in the motion of the traffic agents. We formulate the SMPC problem as a chance-constraint:

$$\min_{\mathbf{U}} \mathcal{J}(\mathbf{x}_0, \mathbf{x}_{ref}, \mathbf{U}) + \mathcal{J}_p(\mathbf{x}_0, \mathbf{x}_{ref}, \mathbf{U}) \quad (11)$$

subjected to:

$$\mathbf{x}_{k+1} = f(\mathbf{x}_k, \mathbf{u}_k) \quad \forall k \in [0, N_p], \quad (12)$$

$$g(\mathbf{x}_k, \mathbf{u}_k) \leq \mathbf{0} \quad \forall k \in [0, N_p], \quad (13)$$

$$Pr[\mathbf{x} \in \mathcal{S}] \leq 1 - \beta \quad \forall k \in [0, N_p] \quad (14)$$

where the aim of the SMPC is to optimize the objective costs \mathcal{J} and \mathcal{J}_p . The dynamics of the ego vehicle (12) is used to predict the future state of the vehicle \mathbf{x}_k , $k = 1, \dots, N_p$ given the current condition \mathbf{x}_0 and the future control inputs $\mathbf{u}_k \in \mathbf{U}$. Constraint (13) are inequality constraints such as limits on the minimum and maximum control inputs. The chance constraint in (14) represents the probabilistic conditions to be satisfied over the future motion of the vehicle given the safe set \mathcal{S} . The SMPC algorithm will guarantee that predefined levels of probability $0 < \beta < 1$ are met for uncertainties in the outcome. Therefore the design parameter β is referred to as the safety level. Note that \mathcal{J} is the objective cost to reach the desired goal and velocity. For brevity, the definition of \mathcal{J} and the constraint are not shown, but can be found in [15]. Here, we define \mathcal{J}_p as the cost to reach the desired F-PIDP setpoints, given that:

$$\mathcal{J}_p = \sum_{k=0}^{N_p} \|d(k) - F_PIDP(k)\|_Q \quad (15)$$

where $d(k)$ is the inter-distance after applying the new control inputs $\mathbf{u}_k \in \mathbf{U}$, while $F_PIDP(k)$ is the reference safety distance (in Section III). The variable Q penalize how well the reference cost is minimized. By minimizing \mathcal{J}_p , SMPC is able to minimize collision risk and ensure comfortable navigation. It is important to mention that, no uncertainties are considered in the SMPC algorithm in order to focus on analyzing the contributions of the proposed

F-PIDP for risk assessment and management during autonomous navigation.

IV. SIMULATION RESULTS AND DISCUSSION

The proposed F-PIDP approach is evaluated through the simulation of two scenarios involving an ego-vehicle and a jaywalking PLEV. The initial state of the ego-vehicle is set to be 15 meters away from the PLEV and with a linear velocity of 5 m/s and 8 m/s respectively. In both scenarios, it is assumed that the ego-vehicle does not have enough time to brake and is expected to perform a swerving maneuver in order to avoid collision with PLEV, ensure the comfort of passengers and also prevent exhibiting highly conservative behaviors.

(cf. video link <https://youtu.be/IS0qhTOYbGc>)

A. Scenario 1: Jaywalking PLEV Switching from Slow to Fast motion

In the first scenario a jaywalking PLEV begins to cross the road at an initial linear velocity of $0.5m/s$ and at an angle equivalent to a right turn (Traj 3 in Figure 5). After approximately 3.9 s there is an abrupt change in the PLEV's behavior, and the velocity increases to 5 m/s (Traj 2 cf. Figure 6). The progress of the probability of each trajectory is shown in Figure 7 b. The sudden switch in behavior is a dangerous situation that will lead to a collision if the ego-vehicle predicts the motion of the PLEV based solely on

the most probable trajectory. This sudden switch in motion from Traj 3(blue) to 2(green) (probability plot cf. Figure 7 b) introduces uncertainty and necessitates an anticipatory assessment of the situation which is achieved using the F-PIDP. Observe that at $t = 0.9s$ the F-PIDP plot (cf. Figure 5) exhibits a convex curve, indicating current safety is satisfactory. However, the high position of the curve from the PIDPs suggests a high risk of future safety distance violations due to Traj 2(green), since it has the minimum PIDP and hence the most dangerous trajectory (cf. Figure 5). This convex form of the F-PIDP results from the fact that Traj 2 has more influence on the position of the pCoM of all the predicted trajectories. As the vehicle moves closer to the PLEV, the F-PIDP takes a concave form even before Traj 2 enters the collision zone (cf. Figure 6). This increases the objective cost of the SMPC thereby suggesting a solution that quickly moves the ego-vehicle away from the collision zone. As earlier mentioned, uncertainties are not added to the SMPC algorithm to reduce its influence on the proposed method. Therefore, collision is avoided with a minimum inter-distance of approximately 1.6 meters away from the PLEV (cf. Figure 8). The ego-vehicle does not decrease its velocity at the beginning because the most dangerous trajectory (Traj 2) has a low probability, hence the velocity plot (cf. Figure 7 a) shows a smooth velocity profile for passenger's comfort even when the ego vehicle accelerates to avoid a collision.

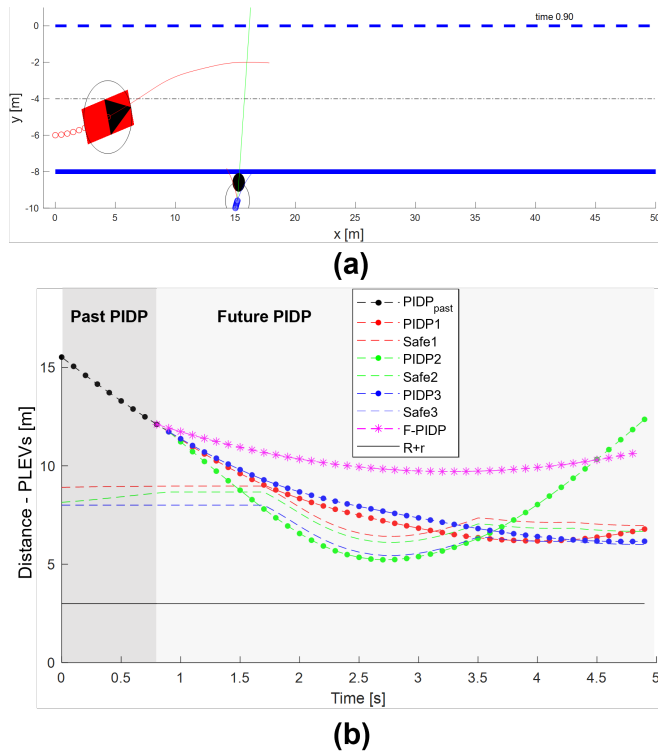


Fig. 5. (a) Scenario 1: Jaywalking PLEV moving Slowly at $t = 0.9s$ (b) Inter-distance plot of ego-vehicle and PLEV: The F-PIDP plot exhibits a convex curve, indicating current safety is satisfactory. However, the steep curve suggests a high risk of future safety distance violations due to PIDP₂

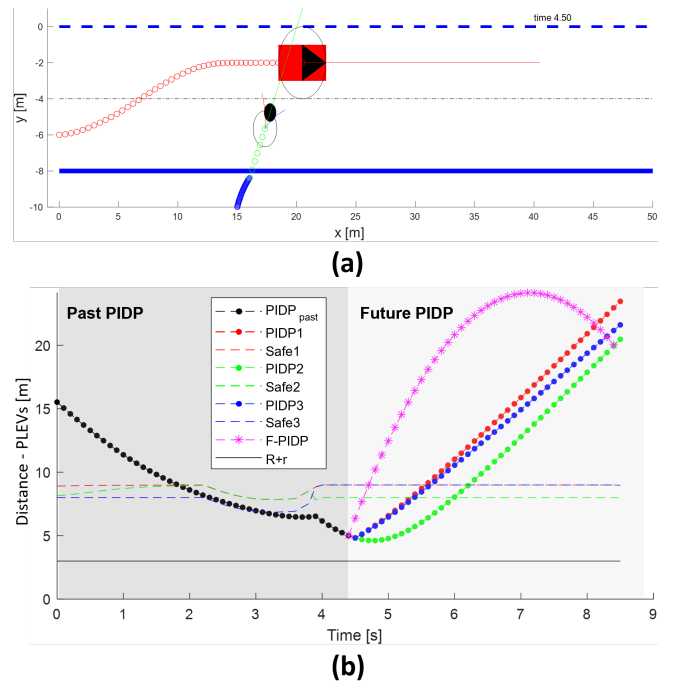


Fig. 6. (a) Scenario 1: Jaywalking PLEV moving Fast at $t = 4.5s$ (b) Inter-distance plot of ego-vehicle and PLEV: As the vehicle moves closer to the PLEV, the F-PIDP takes a concave form even before Traj 2 enters the collision zone

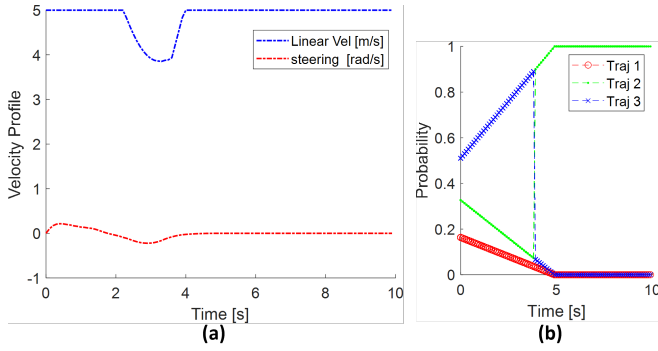


Fig. 7. (a) Velocity plot showing a smooth linear velocity and steering (b) Probability plot with a switching from Traj 3 (blue) to Traj 2 (green) after $t = 3.9s$

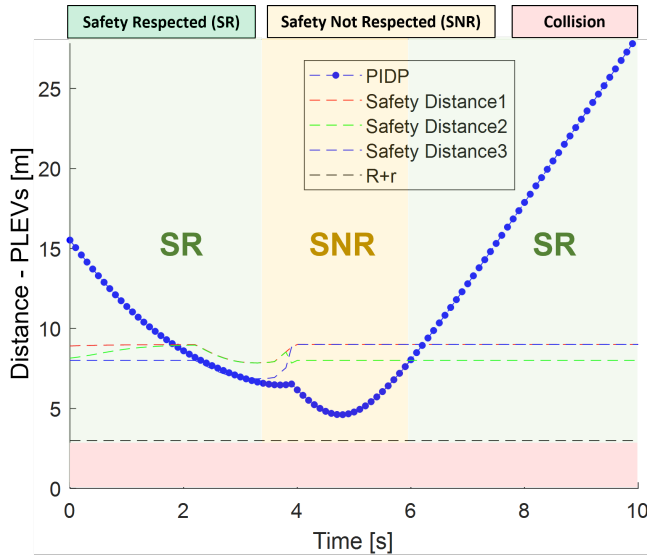


Fig. 8. The overall inter-distance plot of ego-vehicle and PLEV for scenario 1: shows the region where safety is not respected (SNR) when the PLEV changes its trajectory from Traj 3 to 2

B. Scenario 2: PLEV overtaking a parked vehicle

In this scenario, the PLEV attempts to overtake a stationary truck, and in the process, comes dangerously close to the ego vehicle in the adjacent lane. An initial assessment of the scene using PIDP suggest a high risk of collision as indicated by $PIDP_1$ falling below the collision margin (cf. Figure 9). However, the F-PIDP does not only consider the most dangerous trajectory but also considers the most probable trajectory of the PLEV based on the likelihood of each trajectory shown in the probability plot (cf. Figure 10 b). Therefore, the inter-distance plot indicates that the safety distance is respected in the initial few seconds as the ego-vehicle approaches the PLEV (cf. Figure 11). Whereas, during the time interval from $t = 2.6s$ and $t = 8.1s$, the safety distance is temporarily not respected due to the parallel motion of the ego-vehicle and the PLEV (cf. Figure 11). To navigate this risk, the adaptive behavior of the F-PIDP encourages the ego-vehicle to further reduce its speed and slowly approach the PLEV. The F-PIDP plot has a

concave curve that makes it easier for the car to get out of the dangerous situation as shown in Figure 9. This ensures that the ego vehicle neither comes to a complete halt nor makes abrupt maneuvers, but instead, decelerates and then carefully moves past the risky zone. This adaptive response is visualized in the velocity profile plot (cf. Figure 10). Observe that the velocity of the ego-vehicle decreases to about $2m/s$ at time $t = 4.5s$ before it accelerates to move past the PLEV.

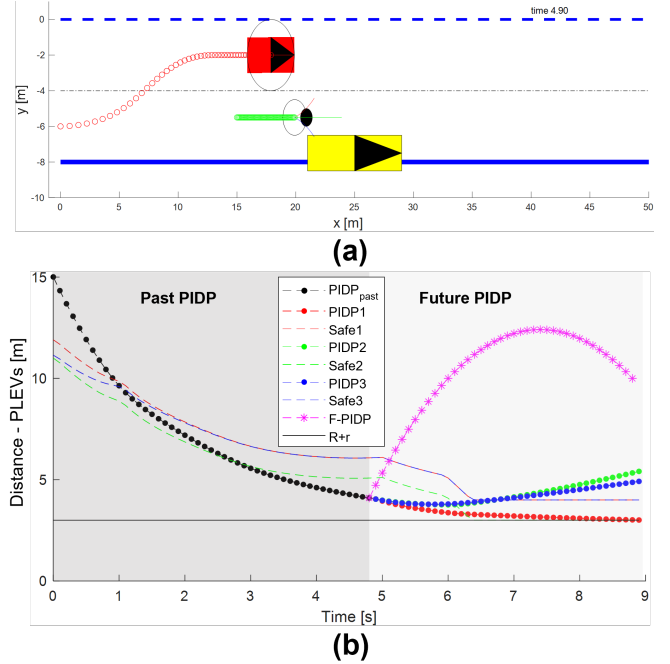


Fig. 9. (a) Scenario 2: PLEV overtaking a parked vehicle at $t = 4.9s$ (b) Inter-distance plot of ego-vehicle and PLEV overtaking a stationary truck: the F-PIDP plot shows a concave curve that encourages escaping from the risky scenario

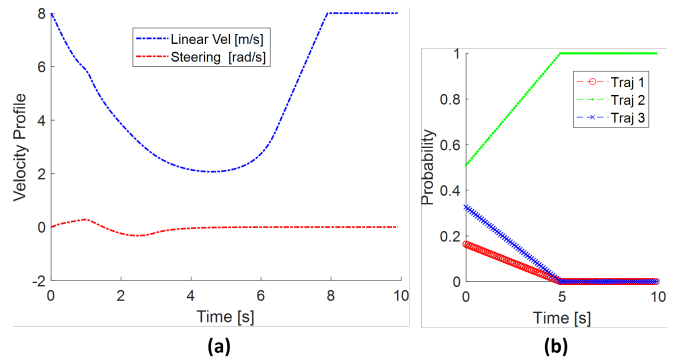


Fig. 10. (a) Velocity plot showing a smooth linear velocity and steering (b) Probability plot with increasing probability for Traj 2 (green)

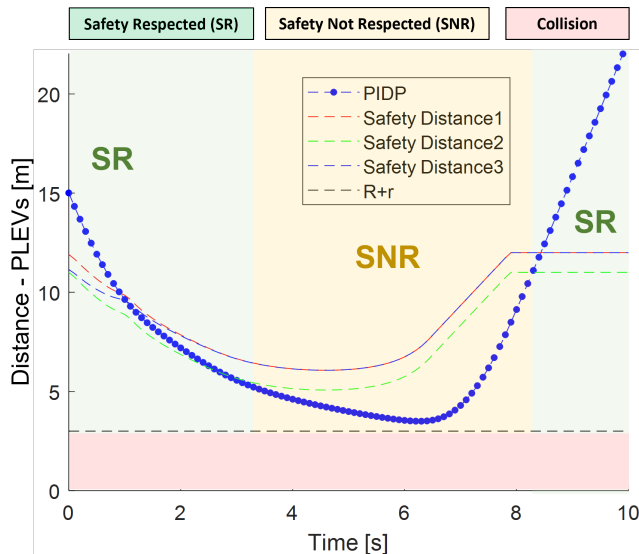


Fig. 11. Inter-distance plot showing the overall PIDP: collision is avoided and the vehicle is able to move into the Safety Respected region (SR)

V. CONCLUSIONS

This paper proposed to perform continuous risk assessment in the presence of PLEVs using a fusion of predictive inter-distance profile (F-PIDP). The F-PIDP method fuses multiple motion intentions (PIDPs) while accounting for the uncertainties in the predicted motion of the PLEV. The fusion involves fitting a quadratic polynomial to key points from all PIDPs and shifting the curve to a desired safety distance. By utilizing the predictions from the F-PIDP, a SMPC algorithm is able to minimize collision risk and ensure comfortable navigation as presented through simulation results. This combination ensures that the ego-vehicle reacts to the current situation and also proactively adjusts its trajectory in anticipation of potential future risk. Future work will consider situations with multiple PLEVs and uncertainties in the predicted velocities of the PLEVs.

ACKNOWLEDGMENT

This research is part of the ANNAPOLIS project (<https://project.inria.fr/annapolis/>), funded by the French National Research Agency (ANR-21-CE22-0014). This work also received the support of the French government, through the CPER RITMEA, Hauts-de-France region.

REFERENCES

- [1] A. Rudenko, L. Palmieri, M. Herman, K. M. Kitani, D. M. Gavrilu, and K. O. Arras, "Human motion trajectory prediction: A survey," *The International Journal of Robotics Research*, vol. 39, no. 8, pp. 895–935, 2020.
- [2] D. Shin, S. Yi, K.-m. Park, and M. Park, "An interacting multiple model approach for target intent estimation at urban intersection for application to automated driving vehicle," *Applied Sciences*, vol. 10, no. 6, p. 2138, 2020.
- [3] F. Warg, M. Skoglund, A. Thorsén, R. Johansson, M. Brännström, M. Gyllenhammar, and M. Sanfridson, "The quantitative risk norm—a proposed tailoring of hara for ads," in *2020 50th Annual IEEE/IFIP International Conference on Dependable Systems and Networks Workshops (DSN-W)*. IEEE, 2020, pp. 86–93.

- [4] J. Li, B. Dai, X. Li, X. Xu, and D. Liu, "A dynamic bayesian network for vehicle maneuver prediction in highway driving scenarios: Framework and verification," *Electronics*, vol. 8, no. 1, p. 40, 2019.
- [5] L. Westhofen, C. Neurohr, T. Koopmann, M. Butz, B. Schütt, F. Utesch, B. Neurohr, C. Gutenkunst, and E. Böde, "Criticality metrics for automated driving: A review and suitability analysis of the state of the art," *Archives of Computational Methods in Engineering*, vol. 30, no. 1, pp. 1–35, 2023.
- [6] M. Kabtoul, M. Prédhumeau, A. Spalanzani, J. Dugdale, and P. Martinet, "How to evaluate the navigation of autonomous vehicles around pedestrians?" *IEEE Transactions on Intelligent Transportation Systems*, 2023.
- [7] A. Laureshyn, Å. Svensson, and C. Hydén, "Evaluation of traffic safety, based on micro-level behavioural data: Theoretical framework and first implementation," *Accident Analysis & Prevention*, vol. 42, no. 6, pp. 1637–1646, 2010.
- [8] S. Das and A. K. Maurya, "Defining time-to-collision thresholds by the type of lead vehicle in non-lane-based traffic environments," *IEEE Transactions on Intelligent Transportation Systems*, vol. 21, no. 12, pp. 4972–4982, 2019.
- [9] C. Laugier, I. E. Paromtchik, M. Perrollaz, M. Yong, J.-D. Yoder, C. Tay, K. Mekhnacha, and A. Nègre, "Probabilistic analysis of dynamic scenes and collision risks assessment to improve driving safety," *IEEE Intelligent Transportation Systems Magazine*, vol. 3, no. 4, pp. 4–19, 2011.
- [10] D. Ibrakken, L. Adouane, and D. Denis, "Safe autonomous overtaking maneuver based on inter-vehicular distance prediction and multi-level bayesian decision-making," in *IEEE International Conference on Intelligent Transportation Systems (ITSC'18)*, Hawaii-USA, 4-7 Novembre 2018.
- [11] A. Tamke, T. Dang, and G. Breuel, "A flexible method for criticality assessment in driver assistance systems," in *2011 IEEE intelligent vehicles symposium (IV)*. IEEE, 2011, pp. 697–702.
- [12] K. Bellingard, L. Adouane, and F. Peyrin, "Risk assessment and management based on neuro-fuzzy system for safe and flexible navigation in unsignalized intersection," in *2023 IEEE Intelligent Vehicles Symposium (IV)*. IEEE, 2023, pp. 1–7.
- [13] C. Pek, S. Manzinger, M. Koschi, and M. Althoff, "Using online verification to prevent autonomous vehicles from causing accidents," *Nature Machine Intelligence*, vol. 2, no. 9, pp. 518–528, 2020.
- [14] K. Ko, S. Han, M. Choi, and K.-S. Kim, "Integrated path planning and tracking control of autonomous vehicle for collision avoidance based on model predictive control and potential field," in *20th International Conference on Control, Automation and Systems (ICCAS)*. IEEE, 2020, pp. 956–961.
- [15] A. Mesbah, "Stochastic model predictive control: An overview and perspectives for future research," *IEEE Control Systems Magazine*, vol. 36, no. 6, pp. 30–44, 2016.
- [16] J. Kocić, N. Jovičić, and V. Drndarević, "An end-to-end deep neural network for autonomous driving designed for embedded automotive platforms," *Sensors*, vol. 19, no. 9, p. 2064, 2019.
- [17] P. J. Navarro, L. Miller, F. Rosique, C. Fernández-Isla, and A. Gila-Navarro, "End-to-end deep neural network architectures for speed and steering wheel angle prediction in autonomous driving," *Electronics*, vol. 10, no. 11, p. 1266, 2021.
- [18] M.-j. Lee and Y.-g. Ha, "Autonomous driving control using end-to-end deep learning," in *2020 IEEE International Conference on Big Data and Smart Computing (BigComp)*. IEEE, 2020, pp. 470–473.
- [19] S. Indolia, A. K. Goswami, S. P. Mishra, and P. Asopa, "Conceptual understanding of convolutional neural network—a deep learning approach," *Procedia computer science*, vol. 132, pp. 679–688, 2018.
- [20] Z. Zhao, W. Chen, X. Wu, P. C. Chen, and J. Liu, "Lstm network: a deep learning approach for short-term traffic forecast," *IET Intelligent Transport Systems*, vol. 11, no. 2, pp. 68–75, 2017.
- [21] R. Rajamani, *Vehicle dynamics and control*. Springer Science & Business Media, 2011.
- [22] M. Mouad, L. Adouane, D. Khadraoui, and P. Martinet, "Mobile robot navigation and obstacles avoidance based on planning and re-planning algorithm," in *10th International IFAC Symposium on Robot Control (SYROCO'12)*, Dubrovnik - Croatia, 5-7, September 2012.
- [23] D. Ibrakken, L. Adouane, and D. Denis, "Reliable risk management for autonomous vehicles based on sequential bayesian decision networks and dynamic inter-vehicular assessment," in *IEEE Intelligent Vehicles Symposium (IV'19)*, Paris-France, 9-12 June 2019.